Systems/Circuits

μ-Opioid Receptor (Oprm1) Copy Number Influences Nucleus Accumbens Microcircuitry and Reciprocal Social Behaviors

Carlee Toddes,[1] Emilia M. Lefevre,[2] Dieter D. Brandner,[1,3] Lauryn Zugschwert,[4] and Patrick E. Rothwell[2]

[1]Graduate Program in Neuroscience, University of Minnesota, Minneapolis, Minnesota 55455, [2]Department of Neuroscience, University of Minnesota, Minneapolis, Minnesota 55455, [3]Medical Scientist Training Program, University of Minnesota, Minneapolis, Minnesota 55455, and [4]Neuroscience Program and Department of Biology, University of St. Thomas, St. Paul, Minnesota 55105

The μ-opioid receptor regulates reward derived from both drug use and natural experiences, including social interaction, through actions in the nucleus accumbens. Here, we studied nucleus accumbens microcircuitry and social behavior in male and female mice with heterozygous genetic knockout of the μ-opioid receptor (Oprm1$^{+/-}$). This genetic condition models the partial reduction of μ-opioid receptor signaling reported in several neuropsychiatric disorders. We first analyzed inhibitory synapses in the nucleus accumbens, using methods that differentiate between medium spiny neurons (MSNs) expressing the D1 or D2 dopamine receptor. Inhibitory synaptic transmission was increased in D2-MSNs of male mutants, but not female mutants, while the expression of gephyrin mRNA and the density of inhibitory synaptic puncta at the cell body of D2-MSNs was increased in mutants of both sexes. Some of these changes were more robust in Oprm1$^{+/-}$ mutants than Oprm1$^{-/-}$ mutants, demonstrating that partial reductions of μ-opioid signaling can have large effects. At the behavioral level, social conditioned place preference and reciprocal social interaction were diminished in Oprm1$^{+/-}$ and Oprm1$^{-/-}$ mutants of both sexes. Interaction with Oprm1 mutants also altered the social behavior of wild-type test partners. We corroborated this latter result using a social preference task, in which wild-type mice preferred interactions with another typical mouse over Oprm1 mutants. Surprisingly, Oprm1$^{-/-}$ mice preferred interactions with other Oprm1$^{-/-}$ mutants, although these interactions did not produce a conditioned place preference. Our results support a role for partial dysregulation of μ-opioid signaling in social deficits associated with neuropsychiatric conditions.

Significance Statement

Activation of the μ-opioid receptor plays a key role in the expression of normal social behaviors. In this study, we examined brain function and social behavior of female and male mice, with either partial or complete genetic deletion of μ-opioid receptor expression. We observed abnormal social behavior following both genetic manipulations, as well as changes in the structure and function of synaptic input to a specific population of neurons in the nucleus accumbens, which is an important brain region for social behavior. Synaptic changes were most robust when μ-opioid receptor expression was only partially lost, indicating that small reductions in μ-opioid receptor signaling can have a large impact on brain function and behavior.

Received Sep. 17, 2020; revised Feb. 17, 2021; accepted June 21, 2021.

Author contributions: C.T. and P.E.R. designed research; C.T., E.M.L., D.D.B., L.Z., and P.E.R. performed research; C.T., E.M.L., D.D.B., and L.Z. analyzed data; C.T. and P.E.R. wrote the paper.

This research was supported by the University of Minnesota MnDRIVE (Minnesota's Discovery, Research and Innovation Economy) initiative (to E.M.L. and P.E.R.), as well as the National Institutes of Health: Grants MH-122094 (C.T.), DA-007234 (C.T., D.D.B.), DA-052109 (D.D.B.), DA-037279 (P.E.R.), and DA-048946 (P.E.R.). We thank Bailey Remmers and David Leipold for technical assistance; as well as Adrine Kocharian, Marc Pisansky, Cassie Retzlaff, and Brian Trieu for stimulating discussions. We also thank the University of Minnesota Mouse Behavior Core for use of their facilities to conduct behavioral tests, and Drs. Robert Meisel and Paul Mermelstein for generously sharing resources.

The authors declare no competing financial interests.

Correspondence should be addressed to Patrick E. Rothwell at rothwell@umn.edu.

https://doi.org/10.1523/JNEUROSCI.2440-20.2021

Introduction

μ-Opioid receptor activation facilitates reward derived from social interaction and other natural experiences, as well as the abuse liability of exogenous opiate narcotics (Panksepp et al., 1980; Trezza et al., 2010; Darcq and Kieffer, 2018). Agonists with high μ-opioid receptor affinity increase visual attention to faces in humans and enhance social play behavior in juvenile rodents as well as marmosets, while pharmacological blockade of opioid receptors causes deficits in these behaviors (Guard et al., 2002; Chelnokova et al., 2016; Achterberg et al., 2019). μ-Opioid receptor availability in the human nucleus accumbens is regulated by a variety of social circumstances (Hsu et al., 2013, 2015), and intra-accumbal manipulations of μ-opioid receptor activation

can bidirectionally modulate social behavior in rodents (Trezza et al., 2011; Resendez et al., 2013; Smith et al., 2018). These findings are consistent with a general role for μ-opioid receptor activation within the nucleus accumbens in motivated behavior (Baldo and Kelley, 2007; Richard et al., 2013; Castro and Bruchas, 2019).

Dysregulation of μ-opioid receptor signaling may contribute to deficits in social interaction and other motivated behaviors that are a hallmark of neuropsychiatric disorders (Kennedy et al., 2006; Prossin et al., 2010; Pellissier et al., 2018; Ashok et al., 2019; Nummenmaa et al., 2020). Mice with constitutive genetic knockout of the μ-opioid receptor (Oprm1) have behavioral deficits in social affiliation, attachment, and reward, as well as dramatic remodeling of synaptic architecture and gene expression in the nucleus accumbens (Moles et al., 2004; Cinque et al., 2012; Becker et al., 2014). These studies have focused on homozygous Oprm1$^{-/-}$ knock-out mice, but the influence of Oprm1 haploinsufficiency on nucleus accumbens circuitry and social behavior has not been investigated. These are important unexplored issues, because partial loss of μ-opioid receptor function (as modeled by the heterozygous Oprm1$^{+/-}$ genotype) is likely more relevant to functional deficits in human neuropsychiatric disorders.

To investigate these issues, we first evaluated the effects of μ-opioid receptor copy number on nucleus accumbens circuitry, using female and male offspring of Oprm1$^{+/-}$ parents. This design allowed us to compare Oprm1$^{+/-}$ offspring with both Oprm1$^{+/+}$ and Oprm1$^{-/-}$ littermates, permitting direct comparisons among all three genotypes while controlling for parental genotype. Analysis of synaptic gene expression, synaptic transmission, and synapse structure all revealed changes in Oprm1$^{+/-}$ mice, which in some cases were greater than or equal to effects in Oprm1$^{-/-}$ mice. We also differentiated between effects on medium spiny neurons (MSNs) that express dopamine receptor Drd1 (D1-MSNs) or Drd2 (D2-MSNs), since both dopamine receptor subtypes contribute to social behavior but also have unique functions (Aragona et al., 2006; Gunaydin et al., 2014; Manduca et al., 2016). These analyses provided novel information regarding sex differences in the organization of nucleus accumbens inhibitory microcircuits and revealed cell type-specific effects of Oprm1 copy number on D2-MSNs.

To determine whether these changes in nucleus accumbens microcircuits are accompanied by alterations in social behavior, we tested Oprm1 mutant mice on a battery of social behavior assays. To thoroughly evaluate all facets of reciprocal social interaction, we also quantified the social behavior of the wild-type mice interacting with Oprm1 mutants during behavioral testing. Our results show impairments in social behavior of Oprm1$^{+/-}$ as well as Oprm1$^{-/-}$ mice, which in turn change the behavior of wild-type mice in a reciprocal fashion. The abnormal social behavior of Oprm1 mutant mice was also apparent in a real-time social preference test (Shah et al., 2013) where wild-type mice chose to avoid social interaction with Oprm1$^{-/-}$ mice. Conversely, Oprm1$^{-/-}$ mutant mice chose to engage in social interaction with other Oprm1$^{-/-}$ mutants, although this interaction did not produce a conditioned place preference (CPP). Our findings reveal fundamental dissociations between different facets of social behavior and demonstrate that partial reductions of μ-opioid signaling can have large effects on brain function and behavior, which may contribute to social deficits associated with neuropsychiatric conditions.

Materials and Methods

Subjects

Experiments were performed with female and male Oprm1 knock-out mice (Matthes et al., 1996). For electrophysiology and immunohistochemistry analyses, Oprm1 mutant mice were crossed with Drd1a-tdTomato BAC transgenic mice (Shuen et al., 2008) and Drd2-eGFP BAC transgenic mice (Gong et al., 2003). All genetically modified strains were maintained on a C57BL/6J genetic background, and distinct groups of wild-type C57BL/6J mice with no Oprm1 mutant ancestry were used as novel stimulus mice for testing social behavior. To avoid ambiguity, we refer to these mice as "C57BL/6J," whereas we refer to wild-type mice generated from Oprm1 breeding colonies as "Oprm1$^{+/+}$." Mice were housed in groups of two to five per cage, on a 12 h light/dark cycle (6:00 A.M. to 6:00 P.M.) at ~23°C with food and water provided *ad libitum*. Experimental procedures were conducted between 10:00 A.M. and 4:00 P.M. and were approved by the Institutional Animal Care and Use Committee of the University of Minnesota.

Table 1. List of primer sequences for quantitative RT-PCR

Gene name	Symbol	Forward oligonucleotide	Reverse oligonucleotide
β-actin	Actb	GACGGCCAGGTCATCACAT	CCACCGATCCACACAGAGTA
μ-Opioid receptor	Oprm1	TCTGCCCGTAATGTTCATGG	AGGCGAAGATGAAGACACAG
Gephyrin	Gphn	GACAGAGCAGTACGTGGAACTTCA	GTCACCATCATAGCCGTCCAA
VGAT	Slc32a1	CTATTCCACATCGCCCTGAT	AATTTGGTGGTGGTGGTGAT
Collybistin	Arhgef9	CCACCTCAGCGAGATAGGAC	GAGCTCCATGCAGGCATCCA
SAP97	Dlg1	CGTAGCTGCGCTGAACTAGA	AGAGCAAAGGGAAGCCAAAT
SAP102	Dlg3	AAGGCAGCAGCTTTCTCTTG	AATCAACACTTCCCGCTCAC
PSD95	Dlg4	AAGCTGGAGCAGGAGTTCAC	GAGGTCTTCGATGACACGTT

Gene expression

Quantitative RT-PCR was performed on nucleus accumbens tissue punches containing the core and shell subregions, as previously described (Lefevre et al., 2020). Tissue was snap frozen on dry ice and stored at −80°C. RNA was isolated using the RNeasy Mini Kit (Qiagen) according to the manufacturer instructions. All RNA samples had an A260/A280 purity ratio ≥2. Reverse transcription was performed using Superscript III (Thermo Fisher Scientific). For each sample, duplicate cDNA preparations were set up. Mouse β-actin mRNA was used as the endogenous control to measure differences in the expression of Oprm1, Gphn, Slc32a1, Arhgef9, Dlg1, Dlg3, and Dlg4. Primer sequences for measurement of each mRNA can be found in Table 1. Quantitative RT-PCR using SYBR green (Bio-Rad) was conducted with a Lightcycler 480 II (Roche) system with the following cycle parameters: 1× 30 s at 95°C, 35× 5 s at 95°C, followed by 30 s at 60°C. Data were analyzed by comparing the C(t) values of the treatments tested using the ΔΔC(t) method. Expression values of target genes were first normalized to the expression value of β-actin. The mean of cDNA replicate reactions was used to quantify the relative target gene expression.

Behavioral responses to morphine administration

Measurement of thermal antinociception and open field locomotion after morphine administration were performed as previously described (Lefevre et al., 2020). We tested open-field locomotor activity in a clear Plexiglas arena (model ENV-510, Med Associates) housed within a sound-attenuating chamber. The location of the mouse within the arena was tracked in two dimensions by arrays of infrared beams, connected to a computer running Activity Monitor software (Med Associates). Mice were habituated to the chamber for 1 h the day before initiating drug treatment. The next day, animals were tested in the open field chamber after the injection of saline (subcutaneously). They were then tested on the following doses of morphine (2.0, 6.32, and 20 mg/kg), receiving an incremental increase in dose every day. The session duration varied as a function of dose: 60 min, saline and 2 mg/kg; 90 min, 6.32 mg/kg; or 120 min, 20 mg/kg. To facilitate comparison between sessions of different length, distance traveled is presented in units of meters per hour.

Thermal antinociception was tested on a 55°C hot plate (IITC Life Scientific). The day before initiating drug treatment, mice were habituated to the instrument for 60 s at room temperature. We then established baseline latency to either jump or lift and lick a hindpaw at 55°C. Mice were then tested 30 min after the injection of saline or morphine, with a maximal cutoff of 30 s to prevent tissue damage. The percentage of

maximum possible effect was calculated as (test latency – baseline latency)/(30 s – baseline latency) × 100.

Electrophysiology

Whole-cell voltage-clamp recordings from nucleus accumbens MSNs in acute brain slices were performed as previously described (Pisansky et al., 2019). Parasagittal slices (240 μm) containing the nucleus accumbens were prepared from Oprm1$^{+/+}$, Oprm1$^{+/-}$, and Oprm1$^{-/-}$ mice carrying the Drd1-tdTomato and/or Drd2-eGFP reporter gene. These mice were offspring of Oprm1$^{+/-}$ heterozygous parents and had not undergone any behavioral testing. Mice were anesthetized with isoflurane and decapitated, and the brains were quickly removed and placed in ice-cold cutting solution containing the following (in mM): 228 sucrose, 26 NaHCO3, 11 glucose, 2.5 KCl, 1 NaH_2PO_4-H_2O, 7 $MgSO_4$-$7H_20$, and 0.5 $CaCl_2$-$_2H_2O$. Slices were cut by adhering the lateral surface of the brain to the stage of a vibratome (model VT1000S, Leica) and allowed to recover for a minimum of 60 min in a submerged holding chamber (~25°C) containing artificial CSF (aCSF) containing the following (in mM): 119 NaCl, 26.2 NaHCO3, 2.5 KCl, 1 NaH_2PO_4-H_2O, 11 glucose, 1.3 $MgSO_4$-7H2O, and 2.5 CaCl2-2H2O. Slices were transferred to a submerged recording chamber and continuously perfused with aCSF at a rate of 2 ml/min at room temperature. All solutions were continuously oxygenated (95% O_2/5% CO_2). To pharmacologically isolate miniature IPSCs (mIPSCs), we added TTX (0.5 μM) to block spontaneous activity, and D-APV (50 μM) and NBQX (10 μM) to block NMDARs and AMPARs, respectively.

Whole-cell recordings from MSNs in the nucleus accumbens medial shell were obtained under visual control using infrared-differential interference contrast optics on an Olympus BX51W1 microscope. Red and green fluorescence were used to identify D1-MSNs and D2-MSNs, respectively. Voltage-clamp recordings were made with borosilicate glass electrodes (2–5 MΩ) filled with the following (in mM): 120 CsMeSO4, 15 CsCl, 10 TEA-Cl, 8 NaCl, 10 HEPES, 1 EGTA, 5 QX-314, 4 ATP-Mg, and 0.3 GTP-Na, pH 7.2–7.3. MSNs were voltage clamped at 0 mV to increase the driving force for current flow through $GABA_A$ receptors. Recordings were performed using a MultiClamp 700B amplifier (Molecular Devices), filtered at 2 kHz, and digitized at 10 kHz. Data acquisition and analysis were performed online using Axograph software. Series resistance was monitored continuously, and experiments were discarded if resistance changed by >20%. At least 200 events per cell were acquired in 15 s blocks and detected using a threshold of 5 pA; all events included in the final data analysis were verified by eye.

Immunohistochemistry and confocal microscopy

Oprm1$^{+/+}$, Oprm1$^{+/-}$, and Oprm1$^{-/-}$ mice carrying the Drd2-eGFP reporter gene were deeply anesthetized using sodium pentobarbitol (Fatal-Plus, Vortech Pharmaceuticals) and transcardially perfused with ice-cold 0.01 M PBS followed by ice-cold 4% PFA in 0.01 M PBS. Brains were removed and postfixed for 24 h in 4% PFA in PBS. The following day, brains were rinsed briefly with 0.01 M PBS and sectioned in the coronal plane at 50 μm. Tissue sections were blocked for 1 h in blocking buffer (2% *N*-hydroxysuccinimide, 0.2% Triton X-100, and 0.05% Tween 20 in 0.01 M PBS), exposed to rabbit anti-GFP (1:1000; catalog #ab290, Abcam; to label D2-MSN somata) and mouse anti-gephyrin (1:250; catalog #147077, Synaptic Systems; to label inhibitory synapses), and diluted in blocking buffer. After 24 h at 4°C, sections were rinsed in wash buffer (Tris-buffered saline with 0.1% Tween 20), and exposed to anti-rabbit A488 (1:1000; catalog #ab150073, Abcam) and anti-mouse A647 secondary antibodies (1:1000; catalog #ab150115, Abcam) overnight at 4°C.

Stained tissue sections were imaged on a laser-scanning confocal microscope (model TCS SPE, Leica Microsystems). A minimum of three image stacks per hemisphere were collected from D2-MSNs in the nucleus accumbens of each section, centered on the border between core and medial shell (including both subregions). Image stacks were collected with a Leica 63× HCX PL APO objective with numerical aperture of 1.4, using laser and photomultiplier tube settings optimized for excitation and emission of Alexa Fluor A488 and A647. Digital zoom between 8× and 10×, was applied and stacks were collected at a 2048 × 2048 pixel resolution using a step size of 0.3 μm and 1 airy unit pinhole diameter. Image stacks were imported into Imaris 9.0 (Bitplane), and analyses were conducted on 3D renderings of compiled confocal stacks. A surface object was applied to the A488 channel to produce a surface representing the GFP-expressing somata in the image stack. Using this surface as a mask, the portion of the A647 channel contained within this surface was isolated to restrict our analysis to individual D2-MSNs. The spot detection algorithm (Banovic et al., 2010) was used to detect gephyrin puncta in the masked A647 channel. A second algorithm was applied to restrict spots within 1 μm of the GFP-immunoreactive surface object. Puncta area density was calculated as the ratio of detected A647 spots to area of the surface object.

Assays of social behavior

To evaluate social behavior, we used a battery of previously described assays: social CPP (Panksepp and Lahvis, 2007; Cinque et al., 2012; Dölen et al., 2013); the standard three-chamber test of sociability and preference for social novelty (Nadler et al., 2004); reciprocal social interaction (Terranova and Laviola, 2005); and a real-time preference test for social interaction (Shah et al., 2013). Animals were moved to an isolated testing room 1 h before tests of social behavior. All experiments were conducted at 60–70 luminosity, and at temperature conditions equal to those of the animal housing facility. Experimental sessions were video recorded and, for social CPP and the three-chamber test, behavioral data were analyzed using ANY-maze behavioral tracking software. Dyadic social interaction was hand scored by researchers blind to experimental conditions. With the exception of social CPP (described below), all tests of social behavior involved novel social partners that were not siblings or cage mates.

Social CPP. Mice were weaned at 3 weeks of age into home cages containing three to five littermates and housed on corn-cob bedding. The social CPP procedure began 1 week after weaning to permit comparison with previous studies of Oprm1$^{-/-}$ mice (Cinque et al., 2012). The CPP test apparatus (18 × 10 × 8 inches) was divided into two equally sized zones by a clear plastic wall, with an oval opening (2 × 1.5 inches) at the base. The floor of each zone was covered with a different type of novel bedding (Cellu-Nest or small animal pellet bedding, PetSmart), with the chamber cleaned and fresh bedding added for each mouse. The protocol began with a baseline CPP session, with each mouse tested individually and allowed to freely explore the apparatus for 10 min. Behavior was video recorded and the time spent in each zone was analyzed automatically using ANY-maze behavioral tracking software. After establishing baseline preference for the two different beddings, mice were assigned to receive social conditioning with littermates from the same home cage for 24 h on one type of bedding, followed by 24 h in social isolation on the other type of bedding. The assignment of each bedding to social or isolation conditioning was counterbalanced for an unbiased design. After isolation conditioning, animals were individually returned to the CPP apparatus for a 10 min test session. A "preference score" was calculated by taking the difference between the time spent in the social zone on the test versus baseline.

Three-chamber social test. Mice were tested at 6–8 weeks of age to permit comparison with previous studies of Oprm1$^{-/-}$ mutants (Becker et al., 2014). The test apparatus was a white plastic rectangular box (25 × 15 × 8 inches) consisting of three interconnected chambers. Two identical wire cups were placed on each end of the apparatus. Before testing, mice were habituated to the empty apparatus for 10 min of free exploration. During the sociability test, an age- and sex-matched C57BL/6J stimulus mouse was introduced in one wire cup, whereas the other cup was left empty. The experimental mouse was then allowed to freely explore all three chambers for 10 min. The social memory portion of the test began immediately thereafter, with a novel age- and sex-matched C57BL/6J stimulus mouse introduced into the previously empty wire cup. The experimental mouse was then allowed to freely explore all three chambers for 10 min. All three phases were recorded by a video camera, and the time spent by the experimental mouse in each chamber and in proximity to each cylinder (<2 cm) was measured by ANY-maze tracking software. After each test, the entire apparatus was cleaned with 70% ethanol.

Reciprocal social interaction test. Mice were tested at 6–8 weeks of age to permit comparison with previous studies of Oprm1$^{-/-}$ mutants (Becker et al., 2014). The test apparatus was an opaque white rectangular

box with 1 cm of fresh corn-cob bedding on the floor. Experimental mice (Oprm1 mutants) were introduced to an age- and sex-matched stimulus mouse in the testing apparatus for 10 min. Each stimulus mouse was either a novel C57BL/6J mouse or a novel Oprm1 mutant from a different litter but with the same genotype as the experimental mouse (Becker et al., 2014) and was used as a stimulus mouse for only a single test session. Video recordings of various social behaviors exhibited by experimental and stimulus mice were hand scored by a blinded experimenter using Button Box 5.0 (Behavioral Research Solutions). Social behaviors were categorized into one of the following groups: nose–nose interaction (direct investigation of orofacial region), huddling (stationary sitting next to partner), social exploration (anogenital investigation, social sniffing outside of orofacial region, social grooming), and following (Terranova and Laviola, 2005). The sum of these social behaviors was used for the "total interaction duration." A small number of videos was lost because of technical errors before these specific behaviors could be scored, resulting in a smaller sample size in behavior breakdowns compared with total interaction duration.

Real-time social preference test. This assay was based on a published protocol that allows a "judge" to choose between interacting with a "typical" mouse (Oprm1$^{+/+}$) and an "atypical" mouse (Oprm1 mutant; Shah et al., 2013). To maintain consistency with other assays of social behavior, mice were tested at 6–8 weeks of age, using the same three-chamber social testing apparatus described above. Judges were habituated for 10 min before testing in the empty apparatus. After habituation, two wire cups were placed in either end chamber: one contained the Oprm1$^{+/+}$ mouse, and the other contained either a Oprm1$^{+/-}$ or Oprm1$^{-/-}$ mutant. Judges were then allowed to freely explore the chamber for 30 min. Test sessions were recorded by a video camera and the time the target mouse spent in each chamber and in proximity to each cylinder (<2 cm) was measured by ANY-maze tracking software. After each test, the entire apparatus was cleaned with 70% ethanol.

Experimental design and statistical analyses

Oprm1 mutant mice were generated using three different breeding schemes. The first breeding strategy involved parents that were both Oprm1$^{+/-}$, generating littermate offspring with a mix of all possible genotypes. This strategy was used to generate mice for analysis of gene expression, behavioral responses to morphine, electrophysiology, and immunohistochemistry. However, one drawback of this strategy is that Mendelian inheritance from Oprm1$^{+/-}$ parents leads to a larger number of Oprm1$^{+/-}$ offspring (50%), relative to Oprm1$^{-/-}$ (25%) or Oprm1$^{+/+}$ (25%). For the assessment of social behavior, we needed to obtain large and comparable numbers of all three genotypes. We therefore analyzed social behavior using offspring from Oprm1$^{+/-}$ parents, as well as age-matched offspring of parents that were both Oprm1$^{+/+}$ (generating only Oprm1$^{+/+}$ offspring) or Oprm1$^{-/-}$ (generating only Oprm1$^{-/-}$ offspring). For social behavior experiments, this means that Oprm1$^{+/+}$ mice were raised by parents that were either Oprm1$^{+/+}$ or Oprm1$^{+/-}$, and Oprm1$^{-/-}$ mice were raised by parents that were either Oprm1$^{+/-}$ or Oprm1$^{-/-}$. For each assay of social behavior, we report values obtained from mice of the same genotype generated by different breeding strategies and pool data from different breeding strategies when results are comparable.

Similar numbers of male and female animals were used in all experiments, with sample sizes indicated in figure legends. Individual data points from males (filled circles) and females (open circles) are distinguished in figures. Sex was included as a variable in factorial ANOVA models analyzed using IBM SPSS Statistics version 24, with repeated measures on within-subject factors. The main effects of sex and interactions involving sex were not significant unless noted otherwise. For the main effects or interactions involving repeated measures, the Huynh–Feldt correction was applied to control for potential violations of the sphericity assumption. This correction reduces the degrees of freedom, resulting in noninteger values. Significant interactions are indicated in figures by a red asterisk and were decomposed by analyzing simple effects (i.e., the effect of one variable at each level of the other variable). Significant main effects were analyzed using least significant difference (LSD) *post hoc* tests, denoted by black asterisks above the data. Effect sizes are expressed as partial η-squared (η_p^2) values. The type I error rate was set to $\alpha = 0.05$ (two tailed) for all comparisons. All summary data are displayed as the mean ± SEM.

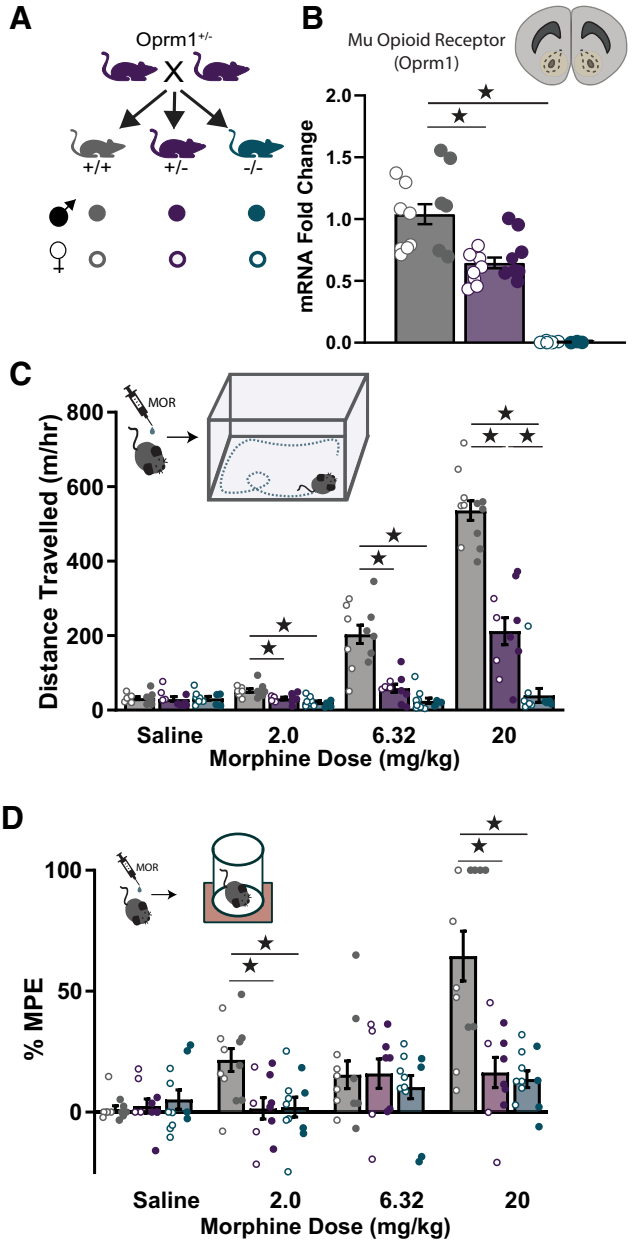

Figure 1. Functional validation of Oprm1 haploinsufficiency. ***A***, Breeding strategy used to generate littermates of all possible genotypes for validation experiments (top), with the legend defining the appearance of individual data points for each genotype and sex (bottom). ***B***, Assessment of μ-opioid receptor (Oprm1) mRNA levels in nucleus accumbens tissue punches using quantitative PCR in Oprm1$^{+/+}$ ($n = 14$), Oprm1$^{+/-}$ ($n = 15$), and Oprm1$^{-/-}$ ($n = 9$) mice. ***C***, ***D***, Distance traveled in a test of open field activity (***C***) and thermal antinociception on the hot plate (***D***) after the injection of morphine in Oprm1$^{+/+}$ ($n = 12$), Oprm1$^{+/-}$ ($n = 10$), and Oprm1$^{-/-}$ ($n = 11$) mice. All groups contained similar numbers of female mice (open symbols) and male mice (closed symbols). $*p < 0.05$ between groups, LSD *post hoc* test.

Results

Functional validation of partial genetic knockout in Oprm1$^{+/-}$ mutant mice

To compare Oprm1$^{+/-}$ and Oprm1$^{-/-}$ mice with Oprm1$^{+/+}$ littermates, we first studied female and male offspring generated by

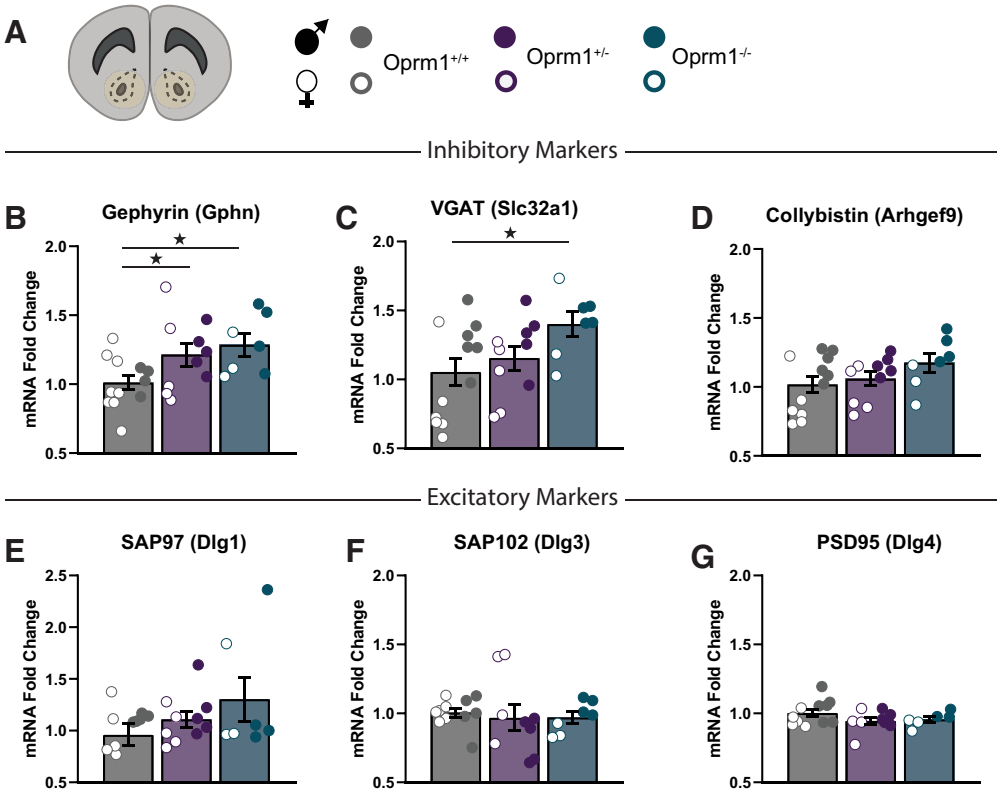

Figure 2. Oprm1 copy number affects synaptic gene expression in the nucleus accumbens. ***A***, The assessment of mRNA levels in nucleus accumbens tissue punches using quantitative PCR (left), with the legend (right) for Oprm1$^{+/+}$ ($n = 12$), Oprm1$^{+/-}$ ($n = 10$), and Oprm1$^{-/-}$ ($n = 7$) mice. ***B–D***, Expression of inhibitory synaptic genes: gephyrin (***B***), VGAT (***C***); and collybistin (***D***). ***E–G***, Expression of excitatory synaptic genes: SAP97 (***E***), SAP102 (***F***), and PSD95 (***G***). All groups contained similar numbers of female mice (open symbols) and male mice (closed symbols). $*p < 0.05$ between groups, LSD *post hoc* test.

breeding two Oprm1$^{+/-}$ parents (Fig. 1*A*). We used quantitative RT-PCR to measure Oprm1 expression in nucleus accumbens tissue punches from all three genotypes (Fig. 1*B*). There was a complete loss of Oprm1 expression in the nucleus accumbens of Oprm1$^{-/-}$ mice, with a partial (~35%) reduction of expression in Oprm1$^{+/-}$ mice ($F_{(2,32)} = 64.19$, $p < 0.001$, $\eta_p^2 = 0.80$). To confirm that this reduction in Oprm1 expression has functional consequences, we injected mice of all three genotypes with ascending doses of morphine, and measured open field activity as well as thermal nociception on a hot plate. In the open field (Fig. 1*C*), Oprm1$^{-/-}$ mice did not exhibit dose-dependent increases in hyperlocomotion, while the behavioral response of Oprm1$^{+/-}$ mice was attenuated but not completely absent (genotype × dose interaction: $F_{(4.33,58.50)} = 48.30$, $p < 0.001$, $\eta_p^2 = 0.78$). On the hot plate (Fig. 1*D*), dose-dependent changes in thermal antinociception were attenuated in both Oprm1$^{-/-}$ and Oprm1$^{+/-}$ mice to a similar extent (genotype × dose interaction: $F_{(6,78)} = 7.38$, $p < 0.001$, $\eta_p^2 = 0.36$). These findings are consistent with those of previous publications (Matthes et al., 1996; Sora et al., 2001) and support the notion that both Oprm1 alleles contribute to the expression of functional receptors (Kieffer and Gavériaux-Ruff, 2002).

Oprm1 copy number affects synaptic gene expression in the nucleus accumbens

Oprm1$^{-/-}$ mice have substantially more symmetrical synapses in the nucleus accumbens, with increased expression of many inhibitory synaptic genes (Becker et al., 2014). We used nucleus accumbens tissue samples to measure mRNA expression of several inhibitory synaptic molecules in all three genotypes (Fig. 2*A*). The expression of gephyrin (Fig. 2*B*), an inhibitory postsynaptic scaffolding protein (Tyagarajan and Fritschy, 2014), was significantly increased in both Oprm1$^{-/-}$ and Oprm1$^{+/-}$ mutants compared with Oprm1$^{+/+}$ controls ($F_{(2,23)} = 3.81$, $p = 0.037$, $\eta_p^2 = 0.25$). The expression of vesicular GABA transporter (VGAT; Fig. 2*C*) was significantly increased in Oprm1$^{-/-}$ mutants ($F_{(2,23)} = 4.06$, $p = 0.031$, $\eta_p^2 = 0.26$). Genotype did not affect the expression of collybistin (Fig. 2*D*), a GDP–GTP exchange factor that facilitates gephyrin trafficking (Kins et al., 2000). However, there was a main effect of sex for the expression of both VGAT ($F_{(1,23)} = 10.33$, $p = 0.004$, $\eta_p^2 = 0.31$) and collybistin ($F_{(1,23)} = 23.47$, $p < 0.001$, $\eta_p^2 = 0.50$), with higher expression of both genes in male mice. We also measured mRNA expression of PSD-95 (Dlg4) and other excitatory synaptic scaffolding molecules in the membrane-associated guanylate kinase family (Won et al., 2017). Oprm1 mutants did not have detectable differences in the expression of Dlg1 (Fig. 2*E*), Dlg3 (Fig. 2*F*), or Dlg4 (Fig. 2*G*). Previous studies found no changes in the number of asymmetrical synapses in the nucleus accumbens of Oprm1$^{-/-}$ mice (Becker et al., 2014), suggesting a stronger influence of Oprm1 copy number on inhibitory synapses in the nucleus accumbens.

Oprm1 copy number affects the function and structure of nucleus accumbens inhibitory synapses

Given the increased expression of inhibitory synaptic genes in Oprm1 mutant mice, we next assessed functional changes in synaptic transmission within the nucleus accumbens. To selectively analyze changes in D1- and D2-MSNs, we crossed Oprm1 knock-out mice with double-transgenic fluorescent reporter

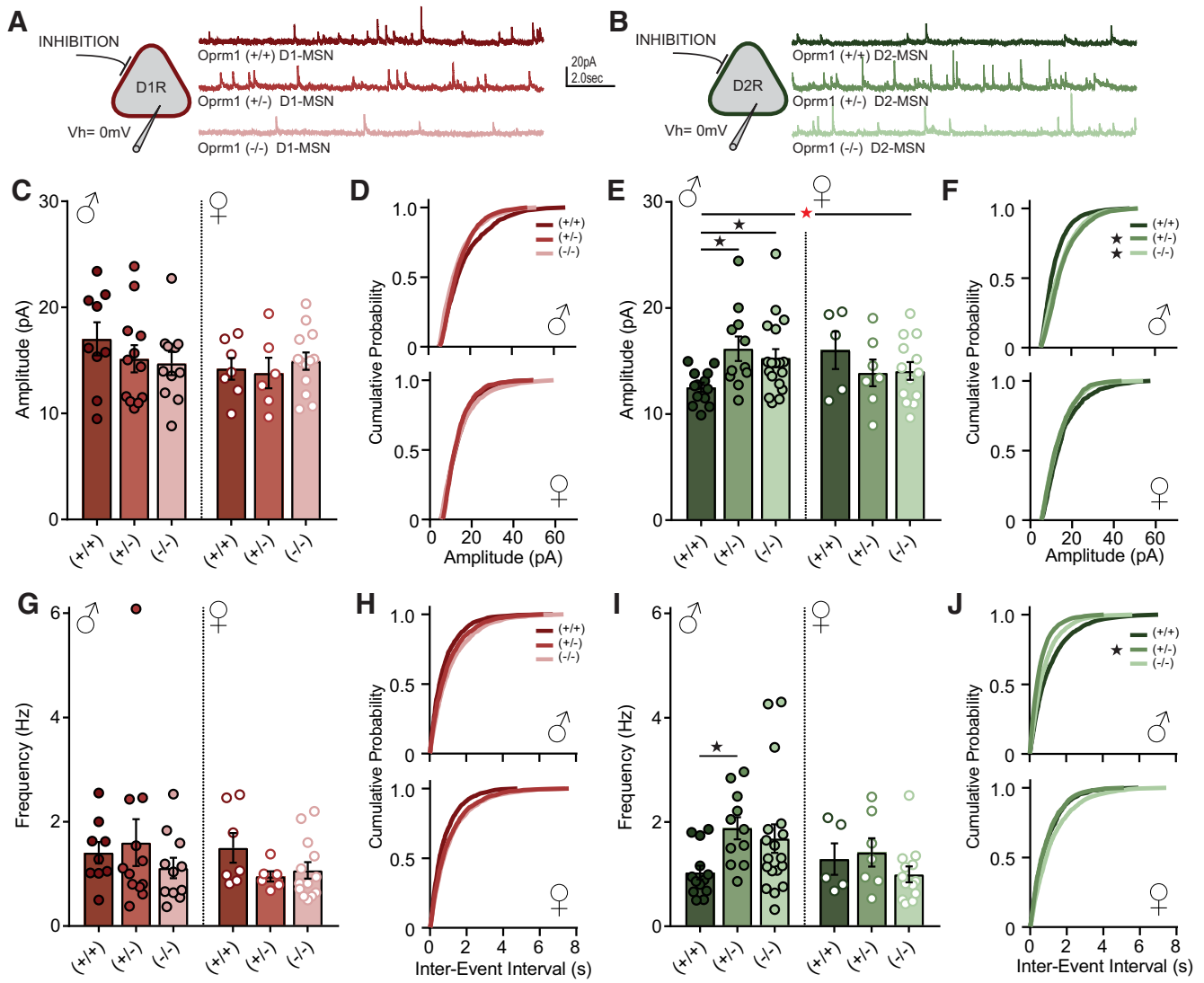

Figure 3. Electrophysiological recordings from MSNs in the nucleus accumbens to assess inhibitory synaptic transmission. ***A***, ***B***, Schematic diagram showing whole-cell voltage-clamp recordings from MSNs identified by the expression of Drd1-tdTomato (***A***) or Drd2-eGFP (***B***). Example traces show mIPSCs recorded for Oprm1$^{+/+}$ (D1, $n = 16$ cells; D2, $n = 18$ cells), Oprm1$^{+/-}$ (D1, $n = 18$ cells; D2, $n = 18$ cells), and Oprm1$^{-/-}$ (D1, $n = 24$ cells; D2, $n = 31$ cells). ***C–F***, Average mIPSC amplitude and cumulative probability plots for D1-MSNs (***C***, ***D***) and D2-MSNs (***E***, ***F***), separated by sex. ***G–J***, Average mIPSC frequency and cumulative probability plots for D1-MSNs (***G***, ***H***) and D2-MSNs (***I***, ***J***), separated by sex. Red asterisk indicates a significant genotype × sex interaction (***E***). $*p < 0.05$ according to LSD *post hoc* test (***E***, ***I***) or Kolmogorov–Smirnov test comparing Oprm1 mutant to control (***F***, ***J***).

mice expressing Drd1-tdTomato and Drd2-eGFP. In acute brain slices prepared from these animals, we performed whole-cell voltage-clamp recordings from red D1-MSNs and green D2-MSNs (Fig. 3*A*,*B*), and measured the frequency and amplitude of mIPSCs. In Oprm1$^{+/+}$ control mice, there was a noteworthy sex difference in basal synaptic transmission (cell type × sex interaction: $F_{(1,30)} = 7.19$, $p = 0.012$, $\eta_p^2 = 0.19$), with larger mIPSC amplitude in male D1-MSNs and female D2-MSNs.

For mIPSC amplitude (Fig. 3*C–F*), omnibus ANOVA revealed a significant cell type × sex × genotype interaction ($F_{(2,113)} = 3.31$, $p = 0.040$, $\eta_p^2 = 0.06$). There were no significant effects on mIPSC amplitude in D1-MSNs (Fig. 3*C*), but for D2-MSNs (Fig. 3*E*) there was a significant sex × genotype interaction ($F_{(2,61)} = 3.62$, $p = 0.033$, $\eta_p^2 = 0.11$). This interaction was driven by a main effect of genotype in male mice ($F_{(2,39)} = 4.52$, $p = 0.017$, $\eta_p^2 = 0.19$), but not in female mice. In D2-MSNs from male mice, mIPSC amplitude was significantly higher in Oprm1$^{+/-}$ and Oprm1$^{-/-}$ mutants relative to Oprm1$^{+/+}$ controls. For mIPSC frequency (Fig. 3*G–J*), there were no significant main effects or interactions in an omnibus ANOVA. However, we noted a trend toward a main effect of genotype in D_2-MSNs from male mice ($F_{(2,39)} = 3.18$, $p = 0.053$, $\eta_p^2 = 0.14$), with higher mIPSC frequency in Oprm1$^{+/-}$ mutants relative to Oprm1$^{+/+}$ controls.

Inhibitory synapses formed at different subcellular locations generate quantal currents with distinct biophysical properties (Koos et al., 2004; Straub et al., 2016). Perisomatic inhibitory synapses generate currents with larger amplitude, while inhibitory synapses in the dendritic arbor generate currents with smaller amplitude (Fig. 4*A*). When we analyzed mIPSC frequency from male D2-MSNs as a function of amplitude (Fig. 4*B*), we found that Oprm1$^{+/-}$ and Oprm1$^{-/-}$ males had a specific increase in the frequency of currents with amplitudes >10 pA (genotype × amplitude interaction: $F_{(2,39)} = 6.13$, $p = 0.005$, $\eta_p^2 = 0.24$), suggesting that Oprm1 copy number affects perisomatic inhibitory synapses. To visualize these synapses, we performed immunohistochemistry for gephyrin in D2-eGFP reporter mice (Gittis et al., 2011), so green fluorescence could be used to construct a soma mask and

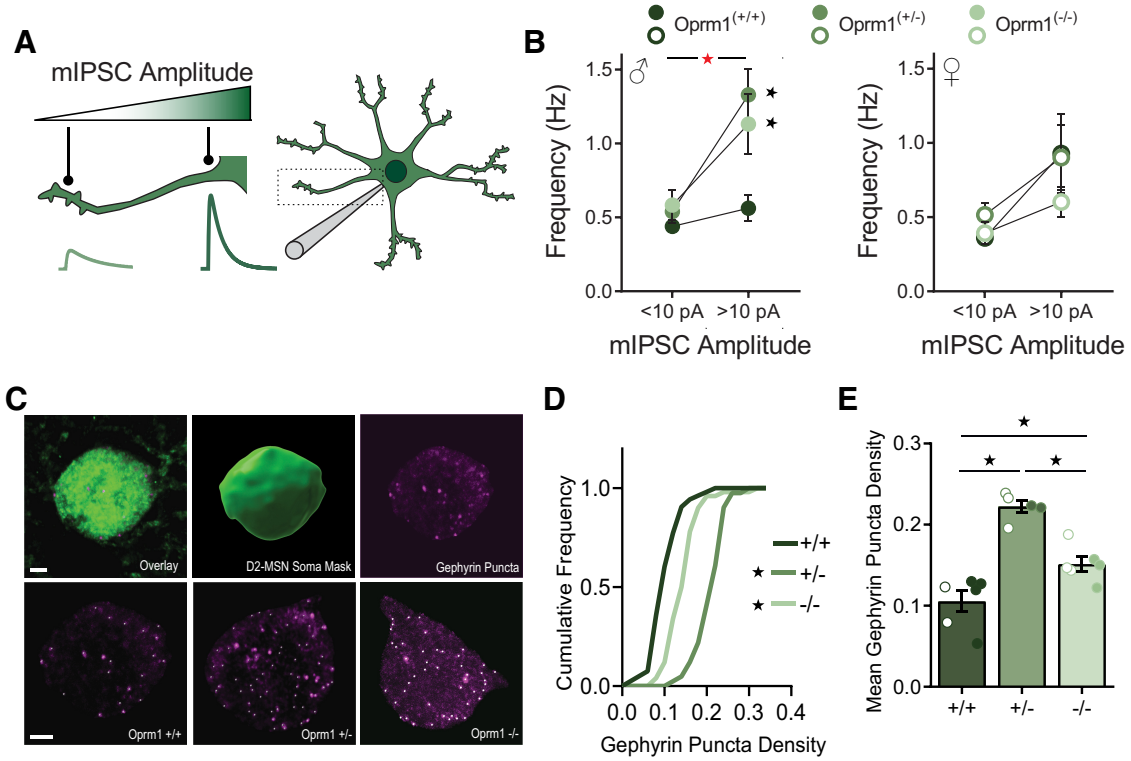

Figure 4. Functional and structural analysis of perisomatic inhibitory synapses in D2-MSNs. ***A***, Schematic diagram showing differences in mIPSC amplitude according to the location of the inhibitory synapses relative to the somatic recording electrode. ***B***, Reanalysis of mIPSC frequency in D2-MSNs from Figure 3, separating event by sex and amplitude: small (<10 pA) or large (>10 pA). ***C***, Examples of confocal images showing D2-eGFP fluorescence (top left) used to create a somatic mask (top middle) for analysis of perisomatic gephyrin-immunoreactive puncta (top right). The bottom row shows representative images for each genotype, with white dots highlighting gephyrin puncta. Scale bars, 2 μm. ***D***, Cumulative probability plot of gephyrin puncta density for D2-MSNs from Oprm1$^{+/+}$ ($n = 250$ cells), Oprm1$^{+/-}$ ($n = 189$ cells), and Oprm1$^{-/-}$ ($n = 223$ cells). ***E***, Mean gephyrin puncta density for D2-MSNs from Oprm1$^{+/+}$ ($n = 6$ mice), Oprm1$^{+/-}$ ($n = 5$ mice), and Oprm1$^{-/-}$ ($n = 6$ mice). All groups contained similar numbers of female mice (open symbols) and male mice (closed symbols). Red asterisk indicates a significant genotype × amplitude interaction (***B***). $*p < 0.05$ comparing Oprm1 mutant to control with LSD *post hoc* test (***B***) or Kolmogorov–Smirnov test (***D***), or LSD *post hoc* test between groups (***E***).

quantify perisomatic gephyrin puncta (Fig. 4*C*,*D*). The mean density of perisomatic gephyrin puncta was doubled in Oprm1$^{+/-}$ mutants (Fig. 4*E*), with a significant but less dramatic increase in Oprm1$^{-/-}$ mutants ($F_{(2,11)} = 24.55$, $p < 0.001$, $\eta_p^2 = 0.82$). Unlike the functional changes in synaptic transmission (Fig. 3), these structural synaptic changes did not appear to differ between sexes, which is consistent with the elevated expression of gephyrin mRNA in nucleus accumbens tissue from both sexes (Fig. 2). Together, our results indicate that Oprm1 copy number alters both the form and function of inhibitory microcircuits in the nucleus accumbens.

Oprm1 copy number alters social reward

Perisomatic inhibitory synapses onto MSNs tend to originate from fast-spiking interneurons (Gittis et al., 2011; Straub et al., 2016). In the nucleus accumbens, fast-spiking interneurons regulate the development of CPP (Wang et al., 2018; Chen et al., 2019), and previous reports indicate that Oprm1$^{-/-}$ mutants fail to develop social CPP (Cinque et al., 2012). To extend this analysis to Oprm1$^{+/-}$ mice, we used a social CPP protocol that began with 24 h of housing with littermates on a distinct bedding material, followed by 24 h of housing in social isolation on a different bedding material (Fig. 5*A*). The preference of individual mice for each bedding material was assessed before and after this conditioning procedure, in sessions we refer to as "baseline" and "test," respectively.

We evaluated social CPP in littermate offspring of Oprm1$^{+/-}$ parents, as well as age-matched offspring of Oprm1$^{+/+}$ or Oprm1$^{-/-}$ parents (Fig. 5*B*). There was a significant session × group interaction ($F_{(4,112)} = 3.85$, $p = 0.006$, $\eta_p^2 = 0.12$), with significant social CPP observed in Oprm1$^{+/+}$ offspring of Oprm1$^{+/+}$ parents (Fig. 5*C*). Social CPP was absent in Oprm1$^{-/-}$ offspring of Oprm1$^{-/-}$ parents, as previously reported (Cinque et al., 2012). Social CPP was also absent in Oprm1$^{-/-}$ and Oprm1$^{+/-}$ offspring of Oprm1$^{+/-}$ parents, suggesting that social reward is diminished by either full or partial loss of Oprm1 signaling. This Oprm1 knock-out mouse line shows intact CPP after exposure to MDMA (3,4-methylenedioxymethamphetamine; Robledo et al., 2004) and cocaine (Contarino et al., 2002; Nguyen et al., 2012), suggesting that the lack of social CPP is not because of a generalized learning or memory deficit. In addition, Oprm1 copy number did not significantly influence social approach or memory in a standard three-chamber test (Table 2). These results provide initial evidence for dissociable mechanisms underlying social approach and social reward.

Somewhat surprisingly, Oprm1$^{+/+}$ offspring of Oprm1$^{+/-}$ parents also failed to exhibit social CPP, although Oprm1$^{+/+}$ offspring of Oprm1$^{+/+}$ parents showed robust CPP (Fig. 5*C*). While this difference could theoretically be related to parental genotype, cross-fostering experiments have shown that parental care by Oprm1 mutants does not alter social behavior of Oprm1$^{+/+}$ mice (Becker et al., 2014). A more likely explanation is that Oprm1$^{+/+}$ offspring of Oprm1$^{+/-}$ parents were conditioned with Oprm1$^{+/-}$ and Oprm1$^{-/-}$ littermates. The abnormal social behavior of mutant littermates could thus have reduced the preference for social bedding that developed in Oprm1$^{+/+}$ mice in a reciprocal fashion.

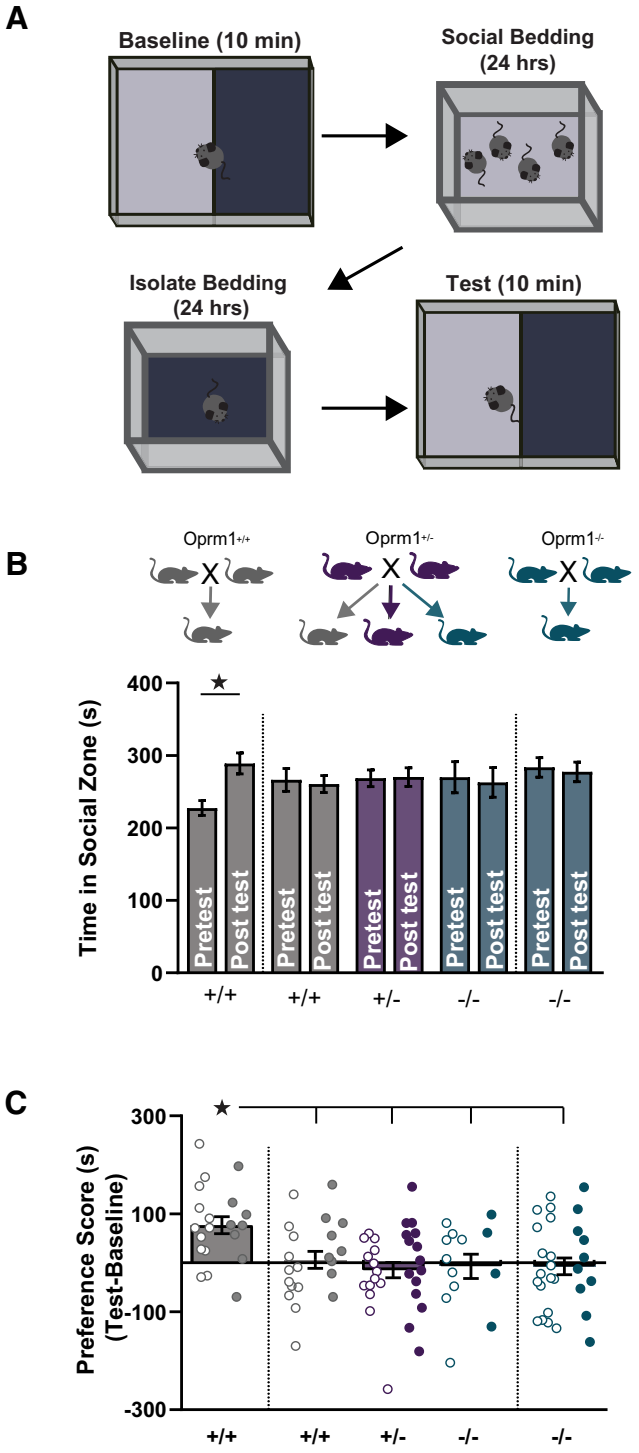

Figure 5. Social CPP as a function of Oprm1 genotype and breeding strategy. ***A***, Schematic diagram of the social CPP protocol. ***B***, Time spent in the social zone for mice of each genotype generated by each breeding strategy ($n = 20/22/29/13/28$, left to right), during the baseline session before conditioning and the test session after conditioning. ***C***, Preference scores for the same groups of mice, calculated as time in the social zone on test minus baseline. Note that +/+ and −/− mice were generated from two different breeding schemes, as shown at the top of panel (***B***). All groups contained similar numbers of female mice (open symbols) and male mice (closed symbols). $*p < 0.05$ according to paired *t* test (***B***) or LSD *post hoc* test (***C***).

Oprm1 copy number alters reciprocal social interaction

We further evaluated reciprocal social interaction between two freely moving age- and sex-matched mice: one mutant animal generated by the Oprm1 breeding strategies described above, and a novel stimulus mouse that was either a mutant mouse of the same genotype or a C57BL/6J wild-type (Fig. 6*A*). The total time spent in social interaction (mean ± SEM) was similar for $Oprm1^{+/+}$ mice interacting with $Oprm1^{+/+}$ (31.0 ± 2.3 s) or C57BL/6J (25.2 ± 3.4 s), and for $Oprm1^{-/-}$ mice interacting with $Oprm1^{-/-}$ (17.4 ± 1.6 s) or C57BL/6J (18.4 ± 1.5 s), so data are pooled for presentation (Fig. 6*B*). There was a main effect of genotype ($F_{(2,166)} = 12.31$, $p < 0.01$, $\eta_p^2 = 0.13$), indicating that both $Oprm1^{+/-}$ and $Oprm1^{-/-}$ mutants spent less time than $Oprm1^{+/+}$ controls engaging in social interaction. The total interaction time was also lower in female mice than male mice (main effect of sex: $F_{(1,166)} = 10.54$, $p < 0.01$, $\eta_p^2 = 0.06$). In this assay, breeding strategy did not appear to influence social behavior: the duration of social interaction (mean ± SEM) was similar in $Oprm1^{+/+}$ mice whose parents were $Oprm1^{+/+}$ (28.0 ± 2.2 s) or $Oprm1^{+/-}$ (28.9 ± 4.6 s), and in $Oprm1^{-/-}$ mice whose parents were $Oprm1^{-/-}$ (19.1 ± 1.85 s) or $Oprm1^{+/-}$ (17.0 ± 1.4 s).

In the reciprocal social interaction test, the total interaction duration includes several qualitatively different types of social behavior (Terranova and Laviola, 2005; Becker et al., 2014). In terms of affiliative social behaviors, there was a main effect of genotype for nose contact (Fig. 6*C*; $F_{(2,129)} = 3.38$, $p = 0.026$, $\eta_p^2 = 0.06$) and huddling (Fig. 6*D*; $F_{(2,129)} = 6.92$, $p = 0.001$, $\eta_p^2 = 0.10$), with decreases in $Oprm1^{-/-}$ mutants that were more moderate in $Oprm1^{+/-}$ mutants, relative to $Oprm1^{+/+}$ controls. In terms of investigative behaviors, there was a main effect of genotype for following (Fig. 6*E*; $F_{(2,129)} = 8.26$, $p < 0.01$, $\eta_p^2 = 0.11$), but no significant change in the amount of other nonreciprocated social exploratory behaviors, such as anogenital sniffing or nose–flank contact (Fig. 6*F*).

In addition to the reciprocal social behavior of the mutant mouse, we also quantified social behavior of the C57BL/6J stimulus mouse in each test session. There was no difference in the total interaction duration as a function of the genotype of the mutant partner (Fig. 6*G*), but interesting trends emerged in the qualitative breakdown of specific types of social behavior. In terms of affiliative social behaviors, there were similar trends toward reduced nose contact and huddling, but not in following (Fig. 6*H–J*). However, C57BL/6J stimulus mice engaged in more nonreciprocated social exploratory behaviors with $Oprm1^{-/-}$ mutant partners (Fig. 6*K*; $F_{(2,83)} = 3.58$, $p = 0.032$, $\eta_p^2 = 0.08$). This result supports the notion that interaction with an Oprm1 mutant mouse changes the social experience of genotypical test partners in a reciprocal manner.

Oprm1 copy number alters real-time social preference

To further assess the preference for social interaction with an Oprm1 mutant mouse versus a typical $Oprm1^{+/+}$ mouse, we measured the choice between these two types of social interaction in real time (Shah et al., 2013). In an initial set of experiments, C57BL/6J mice served as judges in a chamber with two confined stimulus mice (Fig. 7*A*). One of these stimulus mice was typical ($Oprm1^{+/+}$ wild type), while the other stimulus mouse was atypical ($Oprm1^{+/-}$ mutant). Both stimulus mice were age and sex matched to the judge. C57BL/6J judges failed to exhibit reliable discrimination between atypical $Oprm1^{+/-}$ mutants and typical $Oprm1^{+/+}$ controls (Fig. 7*B*,*C*). However, C57BL/6J judges did reliably discriminate between atypical $Oprm1^{-/-}$ mutants and typical $Oprm1^{+/+}$ controls (Fig. 7*D–F*),

Table 2. Social approach and memory of Oprm1 mutant mice in a standard three-chamber test

Genotype	Oprm1$^{+/+}$ (47)	Oprm1$^{+/-}$ (52)	Oprm1$^{-/-}$ (53)
Social approach: time in chamber with C57BL/6J stimulus mouse	292.3 ± 7.3	290.2 ± 7.0	296.8 ± 7.9
Social approach: time in chamber with empty cup	228.0 ± 6.4	229.2 ± 7.0	228.2 ± 7.4
Social approach: time in center chamber	78.2 ± 3.4	80.6 ± 3.0	75.0 ± 4.1
Social approach: statistical results	Chamber: $F_{(1,146)} = 67.25$, $p < 0.001$, $\eta_p^2 = 0.31$ Chamber × genotype: $F_{(12,146)} < 1$		
Social memory: time in chamber with familiar C57BL/6J stimulus mouse	217.6 ± 6.8	223.8 ± 7.9	239.1 ± 8.1
Social memory: time in chamber with novel C57BL/6J stimulus mouse	281.6 ± 6.7	263.0 ± 8.4	257.4 ± 8
Social memory: time in center chamber	100.8 ± 4.4	103.1 ± 4.2	100.2 ± 5.6
Social memory: statistical results	Chamber: $F_{(1,146)} = 18.19$, $p < 0.001$, η_p^2=0.11 Chamber × genotype: $F_{(2,146)} = 2.47$, $p = 0.088$		

All data are presented as the mean ± SEM; the numbers in parentheses represent sample sizes for each genotype.

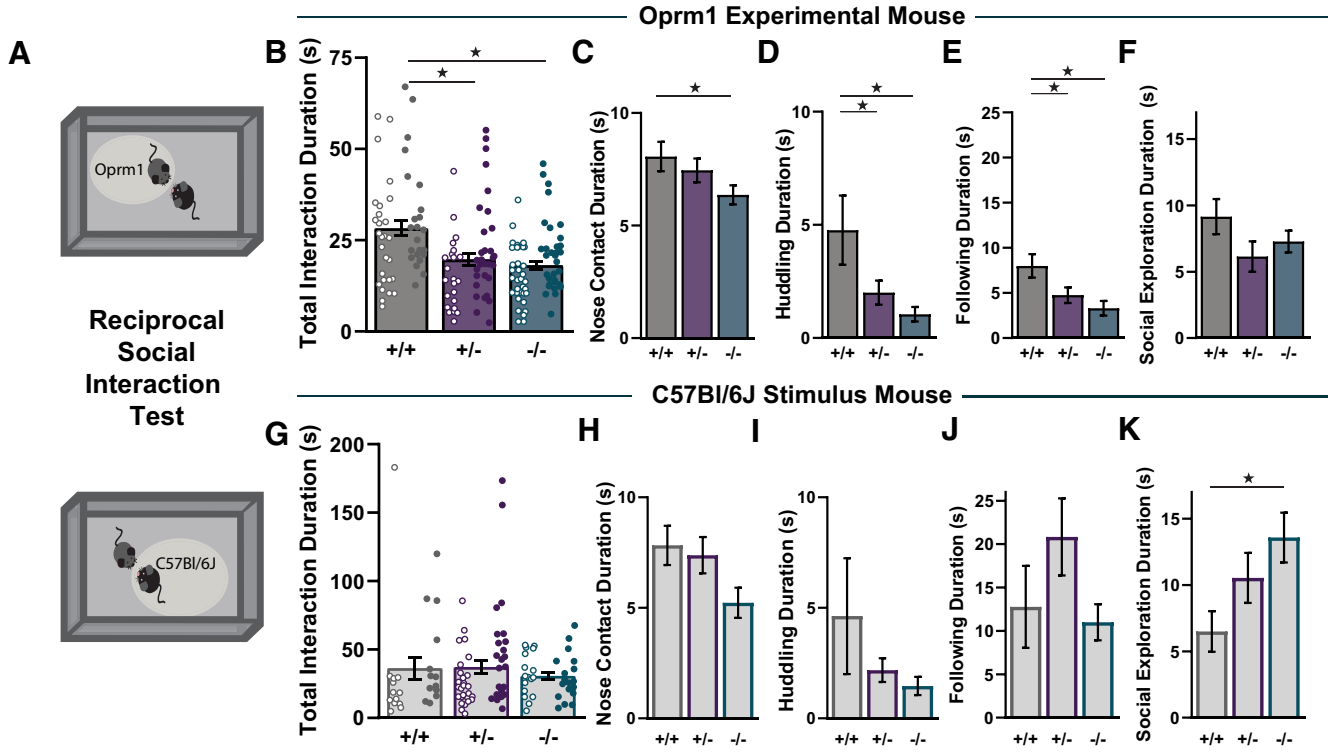

Figure 6. Oprm1 copy number influences on reciprocal social interaction. ***A***, Schematic diagram of the reciprocal social interaction test, separately highlighting behavior of the Orpm1 experimental mouse (top) and the C57BL/6J stimulus mouse (bottom). ***B***, Total interaction durations for Oprm1$^{+/+}$ ($n = 51$), Oprm1$^{+/-}$ ($n = 54$), and Oprm1$^{-/-}$ ($n = 67$). ***C–F***, Duration of nose contact (***C***), huddling (***D***), following (***E***), and social exploration (***F***) for Oprm1$^{+/+}$ ($n = 35$), Oprm1$^{+/-}$ ($n = 45$), and Oprm1$^{-/-}$ ($n = 55$). ***G***, Total interaction durations for C57BL/6J stimulus mice interacting with Oprm1$^{+/+}$ ($n = 26$), Oprm1$^{+/-}$ ($n = 50$), and Oprm1$^{-/-}$ ($n = 35$). ***H–K***, Duration of nose contact (***H***), huddling (***I***), following (***J***), and social exploration (***K***) for C57BL/6J stimulus mice interacting with Oprm1$^{+/+}$ ($n = 20$), Oprm1$^{+/-}$ ($n = 41$), and Oprm1$^{-/-}$ ($n = 28$). All groups contained similar numbers of female mice (open symbols) and male mice (closed symbols). $*p < 0.05$ between groups, LSD *post hoc* test.

exhibiting a robust social preference for the chamber containing the typical mouse ($F_{(1,22)} = 5.87$, $p = 0.002$, $\eta_p^2 = 0.21$). These data provide converging evidence that the abnormal social behavior exhibited by Oprm1 mutant mice can negatively influence the reciprocal social preference of genotypical conspecifics.

Since C57BL/6J judges exhibited reliable discrimination between atypical Oprm1$^{-/-}$ mutants and typical Oprm1$^{+/+}$ controls, we used the same experimental setup to test the real-time social preference of judges that were Oprm1 mutants. Oprm1$^{+/-}$ judges failed to discriminate between atypical Oprm1$^{-/-}$ mutants and typical Oprm1$^{+/+}$ controls (Fig. 7*F–H*). In contrast, Oprm1$^{-/-}$ judges did reliably discriminate between atypical Oprm1$^{-/-}$ mutants and typical Oprm1$^{+/+}$ controls (Fig. 7*I–K*). However, these Oprm1$^{-/-}$ judges exhibited a robust social preference for the chamber containing another atypical Oprm1$^{-/-}$ mouse ($F_{(1,11)} = 19.94$, $p = 0.001$, $\eta_p^2 = 0.64$). Oprm1$^{-/-}$ mice did not develop social CPP when housed with other Oprm1$^{-/-}$ mice (Fig. 5), providing further evidence for dissociable mechanisms underlying social approach and social reward. Our results link deficits in μ-opioid receptor signaling with impairment of social reward, rather than social approach, and illustrate how social interaction with Oprm1 mutant mice can affect the behavior of genotypical partners in a reciprocal fashion.

Discussion

Dysregulation of μ-opioid receptor signaling has been reported in a variety of neuropsychiatric disorders that involve altered social behavior (Kennedy et al., 2006; Prossin et al., 2010;

Pellissier et al., 2018; Ashok et al., 2019; Nummenmaa et al., 2020). These conditions likely involve a partial (rather than a complete) dysregulation of μ-opioid receptor signaling, which we have modeled using mice with heterozygous genetic knockout of Oprm1. These mice exhibited changes in the organization of inhibitory microcircuitry within the nucleus accumbens, where μ-opioid receptor activation plays a particularly critical role in social behavior. Haploinsufficiency of μ-opioid receptor signaling led to robust deficits in both social CPP and reciprocal social interaction in Oprm1$^{+/-}$ mice. Furthermore, the reciprocal social behavior of genotypical stimulus mice was also affected by interaction with Oprm1 mutant mice, which represents a novel aspect of social impairments caused by deficient μ-opioid receptor signaling. Partial reductions of μ-opioid receptor signaling can thus have wide-ranging impacts on both neural circuit organization and behavioral output.

Oprm1 copy number and remodeling of nucleus accumbens microcircuitry

The μ-opioid receptor is abundant in the nucleus accumbens (Moskowitz and Goodman, 1984), and its activation can bidirectionally modulate social preference in rodents (Trezza et al., 2011; Resendez et al., 2013; Smith et al., 2018). Homozygous Oprm1 knock-out mice also show a dramatic increase in the number of symmetrical synapses within the nucleus accumbens (Becker et al., 2014). We corroborated this prior report by measuring mRNA expression of inhibitory synaptic molecules and by using gephyrin immunoreactivity as a marker of perisomatic inhibitory synapses onto D2-MSNs. The density of gephyrin puncta was significantly elevated in Oprm1$^{-/-}$ mice, and elevated even further in Oprm1$^{+/-}$ mice, with no evidence of a sex difference. These striking data show that haploinsufficiency of μ-opioid receptor gene expression can cause more dramatic neurobiological changes than complete genetic knockout of Oprm1, perhaps because of compensatory adaptations that occur in the total absence of μ-opioid receptor expression.

In male Oprm1$^{+/-}$ mice, the structural reorganization of inhibitory synapses onto D2-MSNs was accompanied by altered inhibitory synaptic transmission. There was a significant increase in mIPSC amplitude and frequency in D2-MSNs from male Oprm1$^{+/-}$ mice, similar to previous observations in the central amygdala of male Oprm1$^{-/-}$ mice (Kang-Park et al., 2009). The increase in mIPSC frequency was particularly pronounced for events of large amplitude, which likely correspond to the perisomatic synapses detected using gephyrin immunoreactivity. Fast-spiking interneurons tend to form perisomatic inhibitory synapses with large quantal amplitude onto striatal MSNs (Straub et al., 2016), and these interneurons express the μ-opioid receptor in other brain regions (Drake and Milner, 2006; Glickfeld et al., 2008; Krook-Magnuson et al., 2011). This raises the possibility that the loss of μ-opioid receptor expression from presynaptic neurons may contribute to remodeling of inhibitory synapses onto MSNs in male mice, although the μ-opioid receptor is also expressed by postsynaptic MSNs (Banghart et al., 2015; Charbogne et al., 2017). Additional research is needed to determine whether inhibitory microcircuits are regulated by μ-opioid receptor expression in specific nucleus accumbens cell types, as previously shown for responses to exogenous opioid exposure (Cui et al., 2014; Charbogne et al., 2017; Severino et al., 2020).

Paradoxically, functional changes in synaptic transmission were not observed in female Oprm1$^{+/-}$ mice, although both sexes showed a comparable increase in D2-MSN gephyrin puncta density and gephyrin mRNA expression. One potential

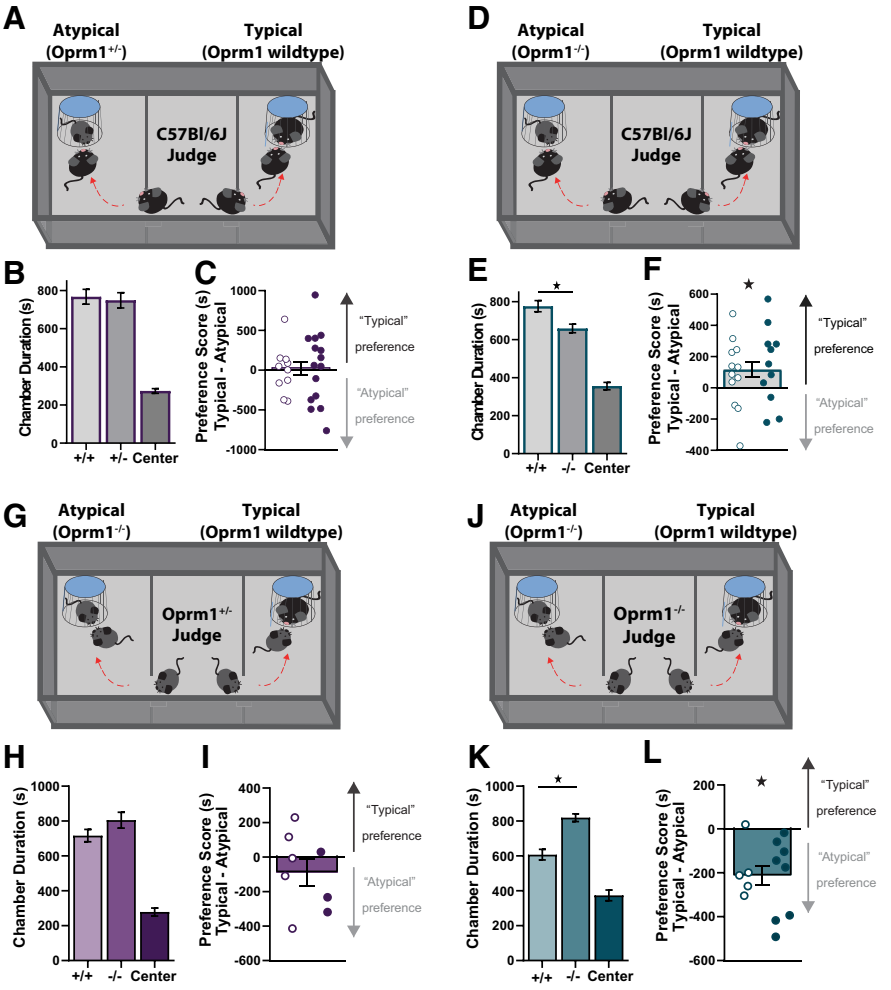

Figure 7. Real-time social preference of C57BL/6J and Oprm1 mutant judges. ***A–C***, C57BL/6J judges ($n = 25$) simultaneously engaging with social targets that are typical (Oprm1$^{+/+}$) or atypical (Oprm1$^{+/-}$), as shown in a schematic diagram (***A***), along with time spent in each chamber (***B***) and preference score (***C***). ***D–F***, C57BL/6J judges ($n = 23$) simultaneously engaging with social targets that are typical (Oprm1$^{+/+}$) or atypical (Oprm1$^{-/-}$), as shown in a schematic diagram (***D***), along with time spent in each chamber (***E***) and preference score (***F***). ***G–I***, Oprm1$^{+/-}$ judges ($n = 8$) simultaneously engaging with social targets that are typical (Oprm1$^{+/+}$) or atypical (Oprm1$^{-/-}$), as shown in a schematic diagram (***G***), along with time spent in each chamber (***H***) and preference score (***I***). ***J–L***, Oprm1$^{-/-}$ judges ($n = 13$) simultaneously engaging with social targets that are typical (Oprm1$^{+/+}$) or atypical (Oprm1$^{-/-}$), as shown in a schematic diagram (***J***), along with time spent in each chamber (***K***) and preference score (***L***). All groups contained similar numbers of female mice (open symbols) and male mice (closed symbols). $*p < 0.05$ according to LSD *post hoc* test (***E***, ***K***) or one-sample *t* test (***F***, ***L***).

explanation for this pattern of results is that the basal mIPSC amplitude is higher in D2-MSNs of female mice and D1-MSNs of male mice. A ceiling effect may therefore have obscured our ability to detect increased mIPSC amplitude in D2-MSNs from female Oprm1 mutant mice. While sex differences at nucleus accumbens inhibitory synapses have not previously been investigated in a cell type-specific fashion, there are well documented sex differences in the structure and function of excitatory synapses in the nucleus accumbens (Forlano and Woolley, 2010; Meitzen et al., 2018), including cell type-specific changes (Cao et al., 2018). We did not detect changes in the mRNA expression of excitatory synaptic scaffolding molecules, and thus did not further evaluate excitatory synaptic transmission in this study. Since inhibitory synaptic transmission appeared relatively normal in female Oprm1$^{-/-}$ mice, changes in excitatory synaptic transmission could make a larger contribution to their atypical social behavior. However, both sexes showed robust changes in gephyrin mRNA expression and D2-MSN gephyrin puncta density, suggesting a common reorganization of inhibitory microcircuitry caused by complete or partial decrements in μ-opioid receptor signaling. It is noteworthy that reductions in sociability caused by social defeat stress are associated with decreased mIPSC frequency in the nucleus accumbens (Heshmati et al., 2020), but this may be because of an effect on D1-MSNs rather than D2-MSNs (Heshmati et al., 2018).

Multifaceted influence of Oprm1 copy number on reciprocal social behavior

Homozygous Oprm1 knock-out mice have deficits in maternal attachment (Moles et al., 2004), social reward (Cinque et al., 2012), and reciprocal social interaction (Becker et al., 2014). We extended these analyses to Oprm1$^{+/-}$ mice using a breeding strategy that permitted comparison with both Oprm1$^{+/+}$ and Oprm1$^{-/-}$ littermates, as well as Oprm1$^{+/+}$ and Oprm1$^{-/-}$ offspring of parents with the same genotype. We found that Oprm1$^{+/-}$ mice had significant reductions in the time spent interacting with novel conspecifics in the reciprocal social interaction test, similar to the phenotype we and others observed in Oprm1$^{-/-}$ mice (Becker et al., 2014). We also analyzed the behavior of genotypical stimulus mice tested with Oprm1 mutant partners in the reciprocal social interaction test. We found subtle indications that interaction with Oprm1 mutant mice alters the reciprocal social behavior of genotypical stimulus mice, as previously reported for other mouse strains with atypical social behavior (Yang et al., 2012).

This notion was further supported by two additional lines of evidence. First, in a test of social CPP, the preference normally observed for group housing with conspecifics was absent when Oprm1$^{+/+}$ mice were housed with Oprm1 mutant littermates. Second, in a test of real-time social preference (Shah et al., 2013), genotypical judges exhibited a preference for interaction with typical Oprm1$^{+/+}$ mice versus atypical Oprm1$^{-/-}$ mice. This preference was not observed when the atypical mouse was Oprm1$^{+/-}$, so heterozygous deletion of the μ-opioid receptor does not completely recapitulate all social phenotypes of homozygous Oprm1 knock-out mice. Our findings are consistent with other reports that the social behavior of genotypical mice can be influenced by atypical conspecifics (Langford et al., 2010; Yang et al., 2012; Heinla et al., 2018; Rogers-Carter et al., 2018).

To our surprise, when Oprm1$^{-/-}$ mice served as judges in the real-time social preference test, they exhibited a preference for other Oprm1$^{-/-}$ mice rather than typical Oprm1$^{+/+}$ mice. We also found that Oprm1$^{-/-}$ exhibited normal levels of social approach in a three-chamber social test (Nadler et al., 2004). These findings differ somewhat from a previous study of the same Oprm1 knock-out mouse on a different genetic background (Becker et al., 2014), but genetic background is known to influence behavior in the three-chamber social test (Moy et al., 2004). It is notable that Oprm1$^{-/-}$ mice do not develop social CPP when housed with other Oprm1$^{-/-}$ littermates (Cinque et al., 2012). This suggests that Oprm1$^{-/-}$ mutants may not enjoy or "like" social interaction with other Oprm1$^{-/-}$ mutants, but still pursue or "want" such interaction. A role for opioid signaling in the hedonic impact of social interaction is consistent with prominent theories of reward (Berridge et al., 2009), which conversely predict that dopamine signaling may mediate the pursuit of social interaction (Gunaydin et al., 2014).

Translational implications

Our findings demonstrate that partial disruption of μ-opioid receptor signaling can have profound effects on both neural circuit organization and behavioral output. In some cases, the impact of haploinsufficiency was even greater than complete loss of μ-opioid receptor signaling. The dysregulation of μ-opioid receptor signaling reported in a variety of neuropsychiatric disorders may therefore reflect fundamental alterations in brain function and contribute to the pathophysiology of these conditions (Kennedy et al., 2006; Prossin et al., 2010; Pellissier et al., 2018; Ashok et al., 2019; Nummenmaa et al., 2020). Partial loss of μ-opioid receptor signaling could be caused by genetic polymorphisms affecting the receptor itself, associated signaling proteins, and opioid peptide ligands as well as their catabolic enzymes. Conversely, genetic variants that enhance some aspects of μ-opioid receptor signaling (like the Oprm1 A118G polymorphism) can increase sociability, even in the heterozygous state (Barr et al., 2008; Copeland et al., 2011; Troisi et al., 2011; Briand et al., 2015). A similar enhancement of endogenous opioid signaling may be possible via pharmacological inhibition of the enzymes that normally degrade endogenous opioid peptides (Roques et al., 2012) or through positive allosteric modulation of the μ-opioid receptor (Kandasamy et al., 2021). Therefore, signaling via the μ-opioid receptor may not only contribute to the etiology of neuropsychiatric disorders, but also represent a target for therapeutic intervention.

References

Achterberg EJM, van Swieten MMH, Houwing DJ, Trezza V, Vanderschuren L (2019) Opioid modulation of social play reward in juvenile rats. Neuropharmacology 159:107332.

Aragona BJ, Liu Y, Yu YJ, Curtis JT, Detwiler JM, Insel TR, Wang Z (2006) Nucleus accumbens dopamine differentially mediates the formation and maintenance of monogamous pair bonds. Nat Neurosci 9:133–139.

Ashok AH, Myers J, Reis Marques T, Rabiner EA, Howes OD (2019) Reduced mu opioid receptor availability in schizophrenia revealed with [^{11}C]-carfentanil positron emission tomographic imaging. Nat Commun 10:4493.

Baldo BA, Kelley AE (2007) Discrete neurochemical coding of distinguishable motivational processes: insights from nucleus accumbens control of feeding. Psychopharmacology (Berl) 191:439–459.

Banghart MR, Neufeld SQ, Wong NC, Sabatini BL (2015) Enkephalin disinhibits mu opioid receptor-rich striatal patches via delta opioid receptors. Neuron 88:1227–1239.

Banovic D, Khorramshahi O, Owald D, Wichmann C, Riedt T, Fouquet W, Tian R, Sigrist SJ, Aberle H (2010) Drosophila neuroligin 1 promotes

growth and postsynaptic differentiation at glutamatergic neuromuscular junctions. Neuron 66:724–738.

Barr CS, Schwandt ML, Lindell SG, Higley JD, Maestripieri D, Goldman D, Suomi SJ, Heilig M (2008) Variation at the mu-opioid receptor gene (OPRM1) influences attachment behavior in infant primates. Proc Natl Acad Sci U S A 105:5277–5281.

Becker JA, Clesse D, Spiegelhalter C, Schwab Y, Le Merrer J, Kieffer BL (2014) Autistic-like syndrome in mu opioid receptor null mice is relieved by facilitated mGluR4 activity. Neuropsychopharmacology 39:2049–2060.

Berridge KC, Robinson TE, Aldridge JW (2009) Dissecting components of reward: "liking", "wanting", and learning. Curr Opin Pharmacol 9:65–73.

Briand LA, Hilario M, Dow HC, Brodkin ES, Blendy JA, Berton O (2015) Mouse model of OPRM1 (A118G) polymorphism increases sociability and dominance and confers resilience to social defeat. J Neurosci 35:3582–3590.

Cao J, Dorris DM, Meitzen J (2018) Electrophysiological properties of medium spiny neurons in the nucleus accumbens core of prepubertal male and female Drd1a-tdTomato line 6 BAC transgenic mice. J Neurophysiol 120:1712–1727.

Castro DC, Bruchas MR (2019) A motivational and neuropeptidergic hub: anatomical and functional diversity within the nucleus accumbens shell. Neuron 102:529–552.

Charbogne P, Gardon O, Martín-García E, Keyworth HL, Matsui A, Mechling AE, Bienert T, Nasseef MT, Robé A, Moquin L, Darcq E, Ben Hamida S, Robledo P, Matifas A, Befort K, Gavériaux-Ruff C, Harsan L-A, von Elverfeldt D, Hennig J, Gratton A, et al. (2017) Mu opioid receptors in gamma-aminobutyric acidergic forebrain neurons moderate motivation for heroin and palatable food. Biol Psychiatry 81:778–788.

Chelnokova O, Laeng B, Løseth G, Eikemo M, Willoch F, Leknes S (2016) The μ-opioid system promotes visual attention to faces and eyes. Soc Cogn Affect Neurosci 11:1902–1909.

Chen X, Liu Z, Ma C, Ma L, Liu X (2019) Parvalbumin interneurons determine emotional valence through modulating accumbal output pathways. Front Behav Neurosci 13:110.

Cinque C, Pondiki S, Oddi D, Di Certo MG, Marinelli S, Troisi A, Moles A, D'Amato FR (2012) Modeling socially anhedonic syndromes: genetic and pharmacological manipulation of opioid neurotransmission in mice. Transl Psychiatry 2:e155.

Contarino A, Picetti R, Matthes HW, Koob GF, Kieffer BL, Gold LH (2002) Lack of reward and locomotor stimulation induced by heroin in mu-opioid receptor-deficient mice. Eur J Pharmacol 446:103–109.

Copeland WE, Sun H, Costello EJ, Angold A, Heilig MA, Barr CS (2011) Child μ-opioid receptor gene variant influences parent-child relations. Neuropsychopharmacology 36:1165–1170.

Cui Y, Ostlund SB, James AS, Park CS, Ge W, Roberts KW, Mittal N, Murphy NP, Cepeda C, Kieffer BL, Levine MS, Jentsch JD, Walwyn WM, Sun YE, Evans CJ, Maidment NT, Yang XW (2014) Targeted expression of μ-opioid receptors in a subset of striatal direct-pathway neurons restores opiate reward. Nat Neurosci 17:254–261.

Darcq E, Kieffer BL (2018) Opioid receptors: drivers to addiction? Nat Rev Neurosci 19:499–514.

Dölen G, Darvishzadeh A, Huang KW, Malenka RC (2013) Social reward requires coordinated activity of nucleus accumbens oxytocin and serotonin. Nature 501:179–184.

Drake CT, Milner TA (2006) Mu opioid receptors are extensively co-localized with parvalbumin, but not somatostatin, in the dentate gyrus. Neurosci Lett 403:176–180.

Forlano PM, Woolley CS (2010) Quantitative analysis of pre- and postsynaptic sex differences in the nucleus accumbens. J Comp Neurol 518:1330–1348.

Gittis AH, Hang GB, LaDow ES, Shoenfeld LR, Atallah BV, Finkbeiner S, Kreitzer AC (2011) Rapid target-specific remodeling of fast-spiking inhibitory circuits after loss of dopamine. Neuron 71:858–868.

Glickfeld LL, Atallah BV, Scanziani M (2008) Complementary modulation of somatic inhibition by opioids and cannabinoids. J Neurosci 28:1824–1832.

Gong S, Zheng C, Doughty ML, Losos K, Didkovsky N, Schambra UB, Nowak NJ, Joyner A, Leblanc G, Hatten ME, Heintz N (2003) A gene expression atlas of the central nervous system based on bacterial artificial chromosomes. Nature 425:917–925.

Guard HJ, Newman JD, Roberts RL (2002) Morphine administration selectively facilitates social play in common marmosets. Dev Psychobiol 41:37–49.

Gunaydin LA, Grosenick L, Finkelstein JC, Kauvar IV, Fenno LE, Adhikari A, Lammel S, Mirzabekov JJ, Airan RD, Zalocusky KA, Tye KM, Anikeeva P, Malenka RC, Deisseroth K (2014) Natural neural projection dynamics underlying social behavior. Cell 157:1535–1551.

Heinla I, Åhlgren J, Vasar E, Voikar V (2018) Behavioural characterization of C57BL/6N and BALB/c female mice in social home cage – effect of mixed housing in complex environment. Physiol Behav 188:32–41.

Heshmati M, Aleyasin H, Menard C, Christoffel DJ, Flanigan ME, Pfau ML, Hodes GE, Lepack AE, Bicks LK, Takahashi A, Chandra R, Turecki G, Lobo MK, Maze I, Golden SA, Russo SJ (2018) Cell-type-specific role for nucleus accumbens neuroligin-2 in depression and stress susceptibility. Proc Natl Acad Sci U S A 115:1111–1116.

Heshmati M, Christoffel DJ, LeClair K, Cathomas F, Golden SA, Aleyasin H, Turecki G, Friedman AK, Han MH, Menard C, Russo SJ (2020) Depression and social defeat stress are associated with inhibitory synaptic changes in the nucleus accumbens. J Neurosci 40:6228–6233.

Hsu DT, Sanford BJ, Meyers KK, Love TM, Hazlett KE, Wang H, Ni L, Walker SJ, Mickey BJ, Korycinski ST, Koeppe RA, Crocker JK, Langenecker SA, Zubieta JK (2013) Response of the μ-opioid system to social rejection and acceptance. Mol Psychiatry 18:1211–1217.

Hsu DT, Sanford BJ, Meyers KK, Love TM, Hazlett KE, Walker SJ, Mickey BJ, Koeppe RA, Langenecker SA, Zubieta JK (2015) It still hurts: altered endogenous opioid activity in the brain during social rejection and acceptance in major depressive disorder. Mol Psychiatry 20:193–200.

Kandasamy R, Hillhouse TM, Livingston KE, Kochan KE, Meurice C, Eans SO, Li MH, White AD, Roques BP, McLaughlin JP, Ingram SL, Burford NT, Alt A, Traynor JR (2021) Positive allosteric modulation of the mu-opioid receptor produces analgesia with reduced side effects. Biochem Pharmacol U S A 118:e2000017118.

Kang-Park MH, Kieffer BL, Roberts AJ, Roberto M, Madamba SG, Siggins GR, Moore SD (2009) Mu-opioid receptors selectively regulate basal inhibitory transmission in the central amygdala: lack of ethanol interactions. J Pharmacol Exp Ther 328:284–293.

Kennedy SE, Koeppe RA, Young EA, Zubieta JK (2006) Dysregulation of endogenous opioid emotion regulation circuitry in major depression in women. Arch Gen Psychiatry 63:1199–1208.

Kieffer BL, Gavériaux-Ruff C (2002) Exploring the opioid system by gene knockout. Prog Neurobiol 66:285–306.

Kins S, Betz H, Kirsch J (2000) Collybistin, a newly identified brain-specific GEF, induces submembrane clustering of gephyrin. Nat Neurosci 3:22–29.

Koos T, Tepper JM, Wilson CJ (2004) Comparison of IPSCs evoked by spiny and fast-spiking neurons in the neostriatum. J Neurosci 24:7916–7922.

Krook-Magnuson E, Luu L, Lee SH, Varga C, Soltesz I (2011) Ivy and neurogliaform interneurons are a major target of μ-opioid receptor modulation. J Neurosci 31:14861–14870.

Langford DJ, Tuttle AH, Brown K, Deschenes S, Fischer DB, Mutso A, Root KC, Sotocinal SG, Stern MA, Mogil JS, Sternberg WF (2010) Social approach to pain in laboratory mice. Soc Neurosci 5:163–170.

Lefevre EM, Pisansky MT, Toddes C, Baruffaldi F, Pravetoni M, Tian L, Kono TJY, Rothwell PE (2020) Interruption of continuous opioid exposure exacerbates drug-evoked adaptations in the mesolimbic dopamine system. Neuropsychopharmacology 45:1781–1792.

Manduca A, Servadio M, Damsteegt R, Campolongo P, Vanderschuren LJ, Trezza V (2016) Dopaminergic neurotransmission in the nucleus accumbens modulates social play behavior in rats. Neuropsychopharmacology 41:2215–2223.

Matthes HW, Maldonado R, Simonin F, Valverde O, Slowe S, Kitchen I, Befort K, Dierich A, Le Meur M, Dollé P, Tzavara E, Hanoune J, Roques BP, Kieffer BL (1996) Loss of morphine-induced analgesia, reward effect

and withdrawal symptoms in mice lacking the μ-opioid-receptor gene. Nature 383:819–823.
Meitzen J, Meisel RL, Mermelstein PG (2018) Sex differences and the effects of estradiol on striatal function. Curr Opin Behav Sci 23:42–48.
Moles A, Kieffer BL, D'Amato FR (2004) Deficit in attachment behavior in mice lacking the mu-opioid receptor gene. Science 304:1983–1986.
Moskowitz AS, Goodman RR (1984) Light microscopic autoradiographic localization of mu and delta opioid binding sites in the mouse central nervous system. J Neurosci 4:1331–1342.
Moy SS, Nadler JJ, Perez A, Barbaro RP, Johns JM, Magnuson TR, Piven J, Crawley JN (2004) Sociability and preference for social novelty in five inbred strains: an approach to assess autistic-like behavior in mice. Genes Brain Behav 3:287–302.
Nadler JJ, Moy SS, Dold G, Trang D, Simmons N, Perez A, Young NB, Barbaro RP, Piven J, Magnuson TR, Crawley JN (2004) Automated apparatus for quantitation of social approach behaviors in mice. Genes Brain Behav 3:303–314.
Nguyen AT, Marquez P, Hamid A, Kieffer B, Friedman TC, Lutfy K (2012) The rewarding action of acute cocaine is reduced in β-endorphin deficient but not in μ opioid receptor knockout mice. Eur J Pharmacol 686:50–54.
Nummenmaa L, Karjalainen T, Isojärvi J, Kantonen T, Tuisku J, Kaasinen V, Joutsa J, Nuutila P, Kalliokoski K, Hirvonen J, Hietala J, Rinne J (2020) Lowered endogenous mu-opioid receptor availability in subclinical depression and anxiety. Neuropsychopharmacology 45:1953–1959.
Panksepp J, Herman BH, Vilberg T, Bishop P, DeEskinazi FG (1980) Endogenous opioids and social behavior. Neurosci Biobehav Rev 4:473–487.
Panksepp JB, Lahvis GP (2007) Social reward among juvenile mice. Genes Brain Behav 6:661–671.
Pellissier LP, Gandía J, Laboute T, Becker JAJ, Le Merrer J (2018) μ opioid receptor, social behaviour and autism spectrum disorder: reward matters. Br J Pharmacol 175:2750–2769.
Pisansky MT, Lefevre EM, Retzlaff CL, Trieu BH, Leipold DW, Rothwell PE (2019) Nucleus accumbens fast-spiking interneurons constrain impulsive action. Biol Psychiatry 86:836–847.
Prossin AR, Love TM, Koeppe RA, Zubieta JK, Silk KR (2010) Dysregulation of regional endogenous opioid function in borderline personality disorder. Am J Psychiatry 167:925–933.
Resendez SL, Dome M, Gormley G, Franco D, Nevárez N, Hamid AA, Aragona BJ (2013) μ-Opioid receptors within subregions of the striatum mediate pair bond formation through parallel yet distinct reward mechanisms. J Neurosci 33:9140–9149.
Richard JM, Castro DC, Difeliceantonio AG, Robinson MJ, Berridge KC (2013) Mapping brain circuits of reward and motivation: in the footsteps of Ann Kelley. Neurosci Biobehav Rev 37:1919–1931.
Robledo P, Mendizabal V, Ortuño J, de la Torre R, Kieffer BL, Maldonado R (2004) The rewarding properties of MDMA are preserved in mice lacking mu-opioid receptors. Eur J Neurosci 20:853–858.
Rogers-Carter MM, Varela JA, Gribbons KB, Pierce AF, McGoey MT, Ritchey M, Christianson JP (2018) Insular cortex mediates approach and avoidance responses to social affective stimuli. Nat Neurosci 21:404–414.
Roques BP, Fournié-Zaluski MC, Wurm M (2012) Inhibiting the breakdown of endogenous opioids and cannabinoids to alleviate pain. Nat Rev Drug Discov 11:292–310.
Severino AL, Mittal N, Hakimian JK, Velarde N, Minasyan A, Albert R, Torres C, Romaneschi N, Johnston C, Tiwari S, Lee AS, Taylor AM, Gavériaux-Ruff C, Kieffer BL, Evans CJ, Cahill CM, Walwyn WM (2020) μ-Opioid receptors on distinct neuronal populations mediate different aspects of opioid reward-related behaviors. eNeuro 7:ENEURO.0146-20.2020.
Shah CR, Forsberg CG, Kang JQ, Veenstra-Vanderweele J (2013) Letting a typical mouse judge whether mouse social interactions are atypical. Autism Res 6:212–220.
Shuen JA, Chen M, Gloss B, Calakos N (2008) Drd1a-tdTomato BAC transgenic mice for simultaneous visualization of medium spiny neurons in the direct and indirect pathways of the basal ganglia. J Neurosci 28:2681–2685.
Smith CJW, Wilkins KB, Li S, Tulimieri MT, Veenema AH (2018) Nucleus accumbens mu opioid receptors regulate context-specific social preferences in the juvenile rat. Psychoneuroendocrinology 89:59–68.
Sora I, Elmer G, Funada M, Pieper J, Li XF, Hall FS, Uhl GR (2001) Mu opiate receptor gene dose effects on different morphine actions: evidence for differential in vivo mu receptor reserve. Neuropsychopharmacology 25:41–54.
Straub C, Saulnier JL, Bègue A, Feng DD, Huang KW, Sabatini BL (2016) Principles of synaptic organization of GABAergic interneurons in the striatum. Neuron 92:84–92.
Terranova ML, Laviola G (2005) Scoring of social interactions and play in mice during adolescence. Curr Protoc Toxicol Chapter 13: Unit13.10.
Trezza V, Baarendse PJJ, Vanderschuren LJMJ (2010) The pleasures of play: pharmacological insights into social reward mechanisms. Trends Pharmacol Sci 31:463–469.
Trezza V, Damsteegt R, Achterberg EJ, Vanderschuren LJ (2011) Nucleus accumbens μ-opioid receptors mediate social reward. J Neurosci 31:6362–6370.
Troisi A, Frazzetto G, Carola V, Di Lorenzo G, Coviello M, D'Amato FR, Moles A, Siracusano A, Gross C (2011) Social hedonic capacity is associated with the A118G polymorphism of the mu-opioid receptor gene (OPRM1) in adult healthy volunteers and psychiatric patients. Soc Neurosci 6:88–97.
Tyagarajan SK, Fritschy JM (2014) Gephyrin: a master regulator of neuronal function? Nat Rev Neurosci 15:141–156.
Wang X, Gallegos DA, Pogorelov VM, O'Hare JK, Calakos N, Wetsel WC, West AE (2018) Parvalbumin interneurons of the mouse nucleus accumbens are required for amphetamine-induced locomotor sensitization and conditioned place preference. Neuropsychopharmacology 43:953–963.
Won S, Levy JM, Nicoll RA, Roche KW (2017) MAGUKs: multifaceted synaptic organizers. Curr Opin Neurobiol 43:94–101.
Yang M, Abrams DN, Zhang JY, Weber MD, Katz AM, Clarke AM, Silverman JL, Crawley JN (2012) Low sociability in BTBR T+tf/J mice is independent of partner strain. Physiol Behav 107:649–662.